

Coupling High-Throughput and Targeted Screening for Identification of Nonobvious Metabolic Engineering Targets

Mahsa Babaei, Philip Tinggaard Thomsen, Marc Cernuda Pastor, Michael Krogh Jensen, and Irina Borodina*



Cite This: *ACS Synth. Biol.* 2024, 13, 168–182



Read Online

ACCESS |

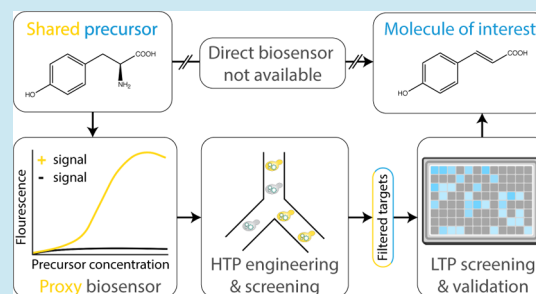
Metrics & More

Article Recommendations

Supporting Information

ABSTRACT: Identification of metabolic engineering targets is a fundamental challenge in strain development programs. While high-throughput (HTP) genetic engineering methodologies capable of generating vast diversity are being developed at a rapid rate, a majority of industrially interesting molecules cannot be screened at sufficient throughput to leverage these techniques. We propose a workflow that couples HTP screening of common precursors (e.g., amino acids) that can be screened either directly or by artificial biosensors, with low-throughput targeted validation of the molecule of interest to uncover nonintuitive beneficial metabolic engineering targets and combinations hereof. Using this workflow, we identified several nonobvious novel targets for improving *p*-coumaric acid (*p*-CA) and *L*-DOPA production from two large 4k gRNA libraries each deregulating 1000 metabolic genes in the yeast *Saccharomyces cerevisiae*. We initially screened yeast cells transformed with gRNA library plasmids for individual regulatory targets improving the production of *L*-tyrosine-derived betaxanthins, identifying 30 targets that increased intracellular betaxanthin content 3.5–5.7 fold. Hereafter, we screened the targets individually in a high-producing *p*-CA strain, narrowing down the targets to six that increased the secreted titer by up to 15%. To investigate whether any of the six targets could be additively combined to improve *p*-CA production further, we created a gRNA multiplexing library and subjected it to our proposed coupled workflow. The combination of regulating *PYC1* and *NTH2* simultaneously resulted in the highest (threefold) improvement of the betaxanthin content, and an additive trend was also observed in the *p*-CA strain. Lastly, we tested the initial 30 targets in a *L*-DOPA producing strain, identifying 10 targets that increased the secreted titer by up to 89%, further validating our screening by proxy workflow. This coupled approach is useful for strain development in the absence of direct HTP screening assays for products of interest.

KEYWORDS: gRNA library, dCas9, *Saccharomyces cerevisiae*, *p*-coumaric acid, betaxanthin, *L*-DOPA

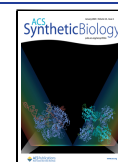


1. INTRODUCTION

High-throughput (HTP) metabolic engineering can uncover novel genetic targets that improve cell factory performance that otherwise would be difficult to arrive at by rational approaches.¹ In contrast to classical mutagenesis, HTP engineering allows manipulation of multiple specific genetic targets at the genomic, transcriptional, or translational levels, thereby generating more focused strain libraries with a higher percentage of phenotypic changes. The techniques that enable HTP engineering of the yeast *Saccharomyces cerevisiae* (*S. cerevisiae*) leverage CRISPR-Cas9² or CRISPR-Cas9-deaminase¹ for genome editing (double- or single-stranded breaks, respectively), catalytically inactive Cas9 endonuclease (CRISPR-dCas9) fused with an activator or repressor for transcriptional regulation,³ or RNAi interference for translational downregulation.⁴ A single transformation can generate 10²–10⁶ yeast strains per μ g of plasmid DNA, depending on the transformation and selection method, e.g., using gRNA vector libraries that can be cost-effectively synthesized on arrays. As demonstrated by Roy et al., gRNA libraries for

targeted genome editing containing the homologous recombination repair fragment besides the gRNA cassette enable robust phenotyping at a large scale in yeast.⁵ The gRNA cassettes themselves can additionally serve as barcodes for identifying the target site in a specific clone or in a pooled group of clones. While HTP engineering methods have been used to uncover novel genotype–phenotype relationships in *S. cerevisiae*, there are few examples of their use for improving the production of small molecules that are not innately fluorescent, pigmented, or coupled to growth.⁶ In fact, the lack of HTP screening assays for most small molecules is a serious obstacle in HTP metabolic engineering, as only a small number of molecules have properties that enable their direct screening

Received: July 3, 2023
Revised: November 28, 2023
Accepted: December 11, 2023
Published: December 23, 2023



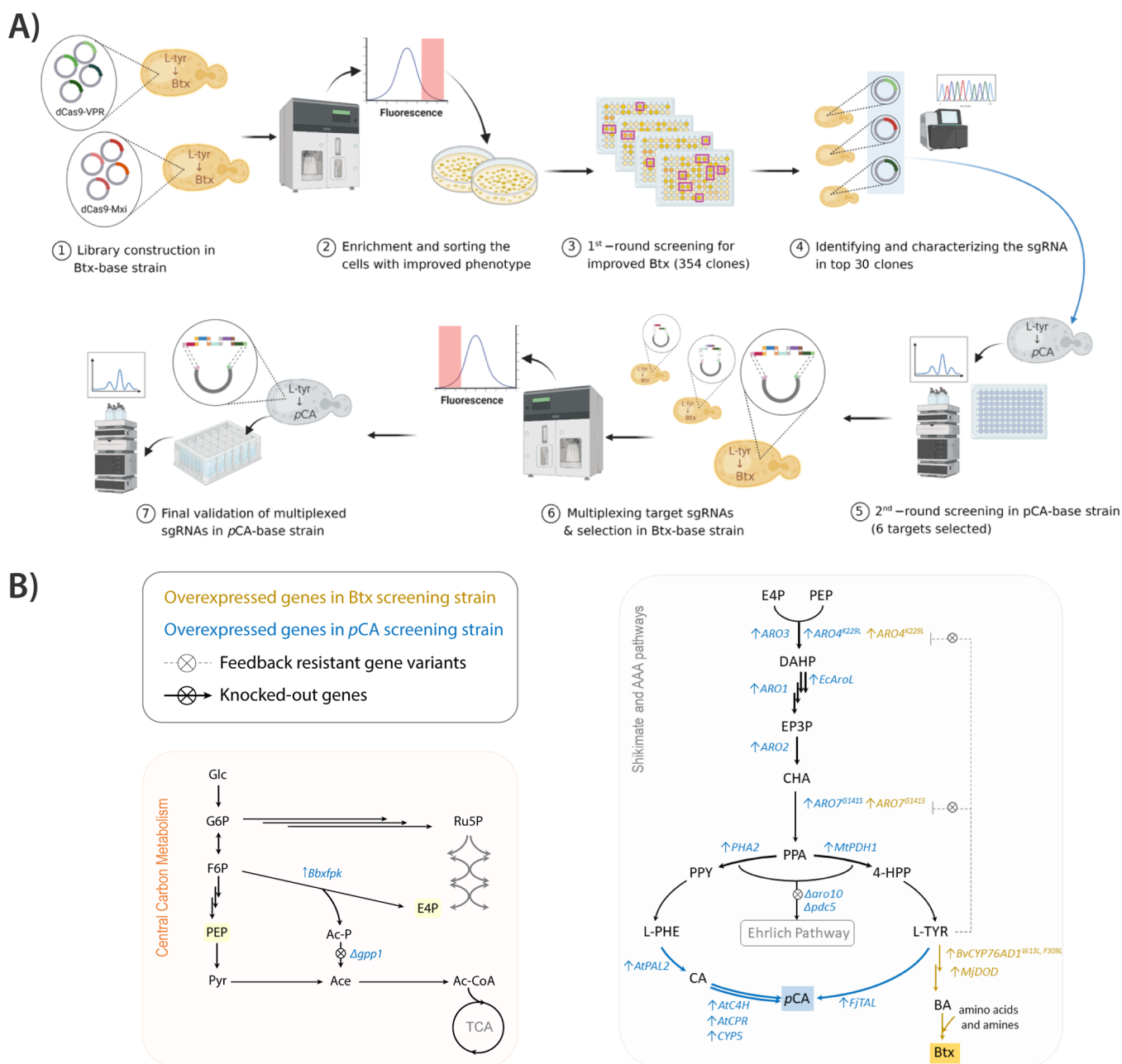


Figure 1. Overview of the study leveraging high-throughput metabolic engineering for the identification of nonintuitive genetic targets for molecules where artificial biosensors are not directly available. (A) Schematic of the bypass workflow implemented for the overproduction of *p*-coumaric acid as a case study. (B) Simplified metabolic pathways for the betaxanthin and *p*-coumaric acid screening strains used in A. The heterologous pathways to *p*-coumaric acid and betaxanthins illustrated together with the rationally engineered genes for both strains are colored blue and yellow, respectively. Abbreviations of the metabolites; Glc, glucose; G6P, glucose-6-phosphate; F6P, fructose-6-phosphate; PEP, phosphoenolpyruvate; Pyr, pyruvate; Ru5P, ribulose 5-phosphate; E4P, erythrose-4-phosphate; Ac-P, acetyl-phosphate; Ace, acetate; Ac-coA, acetyl-CoA; TCA, tricarboxylic acid cycle; DAHP, 3-deoxy-d-arabino-heptulosonate-7-phosphate; EP3P, 5-enolpyruvyl-shikimate-3-phosphate; CHA, chorismic acid; PPA, prephenate; 4-HPP, 4-hydroxyphenylpyruvate; L-TYR, L-tyrosine; PPY, phenylpyruvate; L-PHE, L-phenylalanine; CA, cinnamic acid; *p*CA, *p*-coumaric; BA, betalamic acid; Btx, betaxanthins. Abbreviations of heterologous enzymes (protein accession no.); *Bbxfpk*, *Bifidobacterium breve* fructose-6-P phosphoketolase (WP_101428637); *EcAroL*, *E. coli* shikimate kinase II (P0A6E1); *MtPDH1*, *Medicago truncatula* prephenate dehydrogenase (G7J2F0); *AtPAL2*, *Arabidopsis thaliana* phenylalanine ammonia lyase (P45724); *AtC4H*, *A. thaliana* cinnamate 4-hydroxylase (P92994); *AtCPR*, *A. thaliana* cytochrome P450 reductase 2 (Q9SUM3); *FjTAL*, *Flavobacterium johnsoniae* tyrosine ammonia lyase (A5FKY3); *BvCYP76AD1*^{W13L,F309L}, *Beta vulgaris* cytochrome P450 tyrosine hydroxylase (AET43289.1); *MjDOD*, *Mirabilis japonica* 4,5-DOPA estradiol dioxygenase (B6F0W8.1).

such as color, fluorescence, or an effect on cellular physiology/growth. While artificial biosensors have been developed for a few small molecules that couple the concentration of the compound with the expression of a fluorescent protein, thereby enabling selection by fluorescence-assisted cell sorting

(FACS),⁷ the biosensor development itself remains difficult and time-consuming.^{8,9} Accordingly, analysis for the vast majority of industrially interesting molecules continues to rely on low-throughput (LTP) analytical methods.

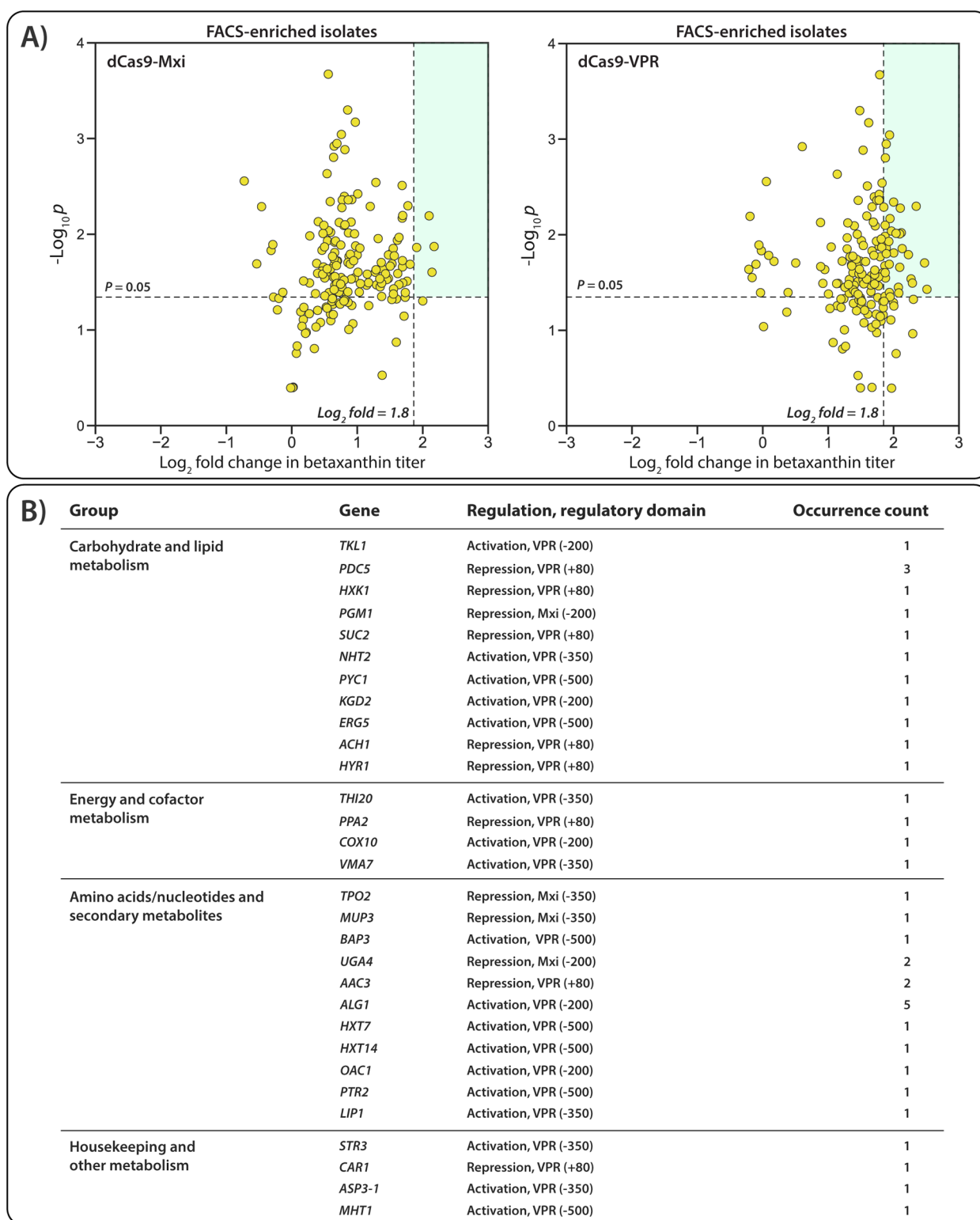


Figure 2. Betaxanthin production by dCas9 yeast libraries and enriched genetic targets. (A) Betaxanthin production by the dCas9-Mxi and dCas9-VPR yeast libraries, plotted as a function of the Log_2 fold change in fluorescence and statistical significance compared to the parent strain. The total number of selected single colonies were 354, and statistical significance was measured using Student's t test (one-tailed; two-sample unequal variance). The selection criteria are shown as green-shaded areas on the graphs. (B) List of sgRNA gene targets as identified by sequencing from the shaded green area in A, their corresponding regulatory domain, and the grouping of the genes based on Bowman et al.³ The selection cutoff was Log_2 fold change >1.8 , and p -value < 0.05 .

In this study, we explored if HTP assays for common precursors (e.g., amino acids) could be useful for identifying nonintuitive targets, and combinations hereof, for improving

small molecule production in yeast for compounds where HTP assays are not directly available. Here, the often less-specific HTP assay serves as an initial filter for library targets relevant

to the biosynthesis of the molecule of interest, which can then be validated by more traditional LTP assays. As a case study, we chose to improve the biosynthesis of *p*-coumaric acid (*p*CA), an aromatic amino acid (AAA)-derived compound that serves as the precursor for many valuable chemicals (Figure 1A). The *p*CA precursors, L-tyrosine, and/or L-phenylalanine, also serve as building blocks for many high-value metabolites that can be produced in yeasts, e.g., flavonoids, stilbenoids, alkaloids, catechol amines, betalains, and others.¹⁰ Well-established rational approaches for improving L-tyrosine and L-phenylalanine supply include relieving feedback inhibition of AAA biosynthetic enzymes, rewiring the central carbon metabolism to increase erythrose-4-phosphate (E4P) supply, and removing degradation via the Ehrlich pathway.^{11–13} *p*CA can be used as a readout for AAA supply, as it can be synthesized directly from L-tyrosine by the action of a single enzyme (tyrosine ammonia-lyase) and/or in two enzymatic steps from L-phenylalanine (phenylalanine ammonia-lyase and cinnamic acid hydroxylase)—together typically not limiting the *p*CA flux.¹⁴ In a rationally engineered *S. cerevisiae* strain, up to 12.5 g/L of *p*CA has been produced in a controlled fed-batch fermentation in bioreactors.¹⁴ To date, no eukaryotic HTP assays have been developed specifically for *p*CA detection.¹⁵ While considerable effort has focused on leveraging a *Bacillus subtilis* *p*CA biosensor expressed in a variety of bacterial hosts and coencapsulated with *p*CA-producing yeast for droplet sorting,^{16,17} such strategies suffer from nonuniform encapsulation and rely on equipment not yet commonplace in most academic facilities. As such, we employed fluorescent betaxanthins (Btx) that are formed by conjugation of L-tyrosine-derived betalamic acid with various amines, including amino acids, as a less-specific but HTP assay for improving the AAA precursor supply to *p*CA.¹⁸ The fluorescent properties of betaxanthins have made them popular signal molecules for improving the production of AAA-derived compounds, e.g., in screening enzyme mutant libraries (library sizes: $\sim 2\text{--}8 \times 10^5$) for improved L-DOPA production,^{18,19} for screening a promoter library (library size: 10^3) for deregulation of phosphofructokinase and pyruvate kinase genes in a *p*CA production strain,¹⁴ and mutants (library size: $> 10^6$) generated by atmospheric and room temperature plasma mutagenesis for improved L-tyrosine titers.²⁰

As our HTP metabolic engineering strategy, we decided to implement CRISPRi/a gRNA libraries created by Bowman et al. that target 969 metabolic genes and titrate their expression by a nuclease-deactivated dCas9 fused to either the transcriptional activator VP64-p65-Rta (VPR) or the repressor Mxi1.³ Hereby, these libraries enable incremental up- and down-regulation of all the metabolic genes in *S. cerevisiae*, including the essential ones.²¹

To identify the targets from the CRISPRi/a gRNA libraries that improve AAA production in yeast, we initially screened the libraries in a betaxanthin-producing strain (see Figure 1B), allowing HTP sorting with FACS, and subsequently screened the enriched targets in a *p*CA-producing strain (see Figure 1B) to validate targets relevant for AAA supply. An overview of the general workflow followed in this study can be found in Figure 1A.

2. RESULTS

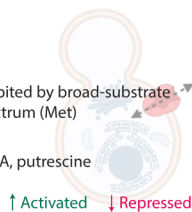
2.1. Identification of 30 Unique Gene Targets Significantly Improving Betaxanthin Production. As a prerequisite for screening the CRISPRi/a gRNA libraries for

targets that might improve *p*CA production, we needed to couple the desired phenotype to a HTP screening and cell sorting method. To the best of our knowledge, there are no yeast-based biosensors available specifically for *p*CA, and so we were curious if betaxanthins could serve as a proxy for AAA supply and by extension *p*CA. Initially, we implemented the betaxanthin expression cassette into the yeast genome to ensure uniform expression across the yeast population (Figure 1B). Hereafter, we expressed feedback-insensitive alleles of the genes *ARO4*^{K229L} and *ARO7*^{G141S} to prevent allosteric inhibition of the DAHP synthase or chorismate mutase by L-tyrosine, resulting in our betaxanthin screening strain (ST9633).²² Betaxanthins are formed from L-tyrosine by an enzymatic conversion into betalamic acid, which then undergoes a spontaneous Schiff-base condensation with amines or amino acids to form this fluorescent (excitation: 463 nm, emission: 512 nm) and yellow-pigmented group of compounds.²³ A list of the isolated and fully characterized betaxanthins found in plants is provided in Supplementary File 1, Figure S1.²⁴ With our betaxanthin screening strain established, we constructed yeast libraries by implementing CRISPRi (dCas9-Mxi1) and CRISPRa (dCas9-VPR) gRNA libraries, respectively. Hereafter, we screened the libraries via FACS, sorting 8,000–10,000 events using a threshold of 1–3% for the library with the highest fluorescence (Figure 1A, step 2). The sorted cells were recovered in mineral media overnight, plated on mineral media agar plates, and then incubated for 4 days to obtain single colonies (see File 1, Figure S2). We visually selected ~ 350 of the most intensely yellow-pigmented colonies (Figure 1A, step 3), cultivated them for 48 h in mineral media (20 g/L glucose) in 96-deep-well plates, and benchmarked their fluorescence against that of the parent strain (ST9633). As seen in Figure 2A, the fluorescence fold change for the dCas9-VPR library (mean = 2.61, median = 2.53, SD = 0.86) was slightly higher than for the dCas9-Mxi1 library (mean = 1.64, median = 1.52, SD = 0.62). Next, we set an arbitrary cutoff at a normalized fluorescence fold change > 3.5 , corresponding to a Log₂ fold change > 1.8 , and *p*-values < 0.05 (the green-shaded area in Figure 2A), resulting in 38 strains, from which we isolated and sequenced the sgRNA plasmids (Figure 1A, step 4). The gene targets and their associated binding sites for the transcriptional regulatory domain can be found in Figure 2B. Surprisingly, there was very little overlap between gene targets, and while *ALG1* (5 isolates) and *PDC5* (3 isolates) were found with the highest frequency, our initial screening resulted in 30 unique gene targets significantly improving betaxanthin production.

2.2. Composition-Dependent Fluorescence Intensity of Betaxanthins Can Lead to False Positives. It is well-established—although arguably under-reported in HTP engineering studies—that an inherent issue with using the group of compounds, termed “betaxanthins” as a proxy for L-tyrosine, is that the fluorescence intensity of the individual betaxanthin molecules is dependent on the functional groups in the amine moiety constituting that particular betaxanthin.²⁵ For instance, Gandia-Herrero et al. have shown that the presence of a carboxylic group in the amine moiety increases the fluorescence intensity of the resulting betaxanthin, while the presence of a hydroxyl group reduces its intensity.²⁶ Furthermore, the fluorescence quantum yield of glutamine-Btx (vulgaxanthin I) is reported to be approximately 2.4-fold higher than that of dopamine-Btx (miraxanthin V).^{27–29} As such, an inherent risk of applying betaxanthin directly as a

A) Amino acid permeases and transporters

Gene	Description	Substrates
↑ <i>Bap3p</i>	Branched-chain amino acid permease	Val, Ile, Phe, Tyr, Trp, Leu, Met, Cys, Thr, Ala
↓ <i>Tpo2p</i>	Polyamine transporter	
↓ <i>Mup3p</i>	Methionine low-affinity permease	Inhibited by broad-substrate spectrum (Met)
↓ <i>Uga4p</i>	GABA permease, vacuole localization	GABA, putrescine



↑ Activated ↓ Repressed

B) Amino acid biosynthesis/catabolism enzymes

Gene	Reaction
<i>STR3</i>	Cystathionine $\xrightarrow{\uparrow \text{Str3p, Irc7p}}$ Homocysteine
<i>MTH1</i>	Homocysteine $\xrightarrow{\uparrow \text{Mth1p, Sam4p}}$ Methionine
<i>CAR1</i>	Arginine $\xrightarrow{\downarrow \text{Car1p}}$ Ornithine
<i>ASP3-1</i>	Asparagine $\xrightarrow{\uparrow \text{Asp-3,1,2,4p}}$ Aspartate



↑ Activated ↓ Repressed

C)

Amine-supplemented betaxanthin cultivation

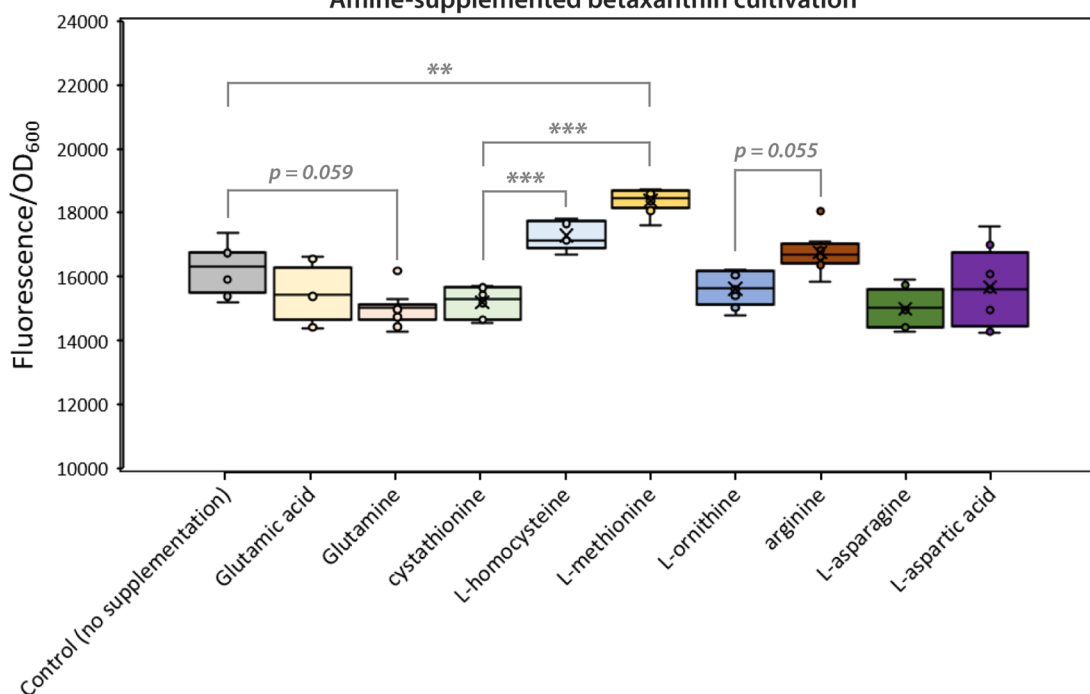


Figure 3. Composition-dependent fluorescence intensity of betaxanthins. (A, B) Classification of targets from Figure 2B classified as permeases/transporters and biosynthetic/catabolic enzymes in amino acid pathways. (C) Normalized fluorescence (to cell growth) for ST9633 growing in modified mineral media (control) or supplemented with 0.5 mM of amines. The data were taken after 48 h of growth for at least $n = 5$ biologically independent samples. Statistical analysis was performed using one-way ANOVA and Tukey's HSD test (* $p < 0.05$, ** $p < 0.01$, *** $p < 0.001$).

readout for AAA (or any other target) in HTP engineering workflows targeting native metabolism is the enrichment of gene perturbations not related to AAA but rather to any of the other betalamate-conjugating amino acids. To investigate if this was leading to false positives in our screening, we grouped the targets from our initial screening into genes acting in transport or biosynthesis/catabolism pathways of amino acids (Figure 3A). Hereafter, we supplemented the specific amino acids reported to be involved in the transport or biosynthesis/catabolism as regulated by those genes to mineral media in order to simulate an increase in their production. The yeast strain used for betaxanthin screening was cultivated in mineral media with or without amino acid supplementation, and clearly the fluorescence measured for equimolar values of different betalamate-conjugating amino acids is different compared to the control strain, with the highest being L-methionine-betaxanthin, and the lowest being L-glutamine-betaxanthin. The comparative fluorescence value of L-methionine > L-homocysteine > cystathionine is a possible explanation for the

enrichment of targets perturbing *BAP3*, *MUP3*, *MTH1*, and *STR3*. A similar explanation could be applied to the enrichment of *ASP3-1*, as aspartate-betaxanthin has more fluorescence intensity than L-asparagine-betaxanthin. Biosensor promiscuity is hardly an issue specific to betaxanthin, in fact most biosensors have imperfect specificity simply due to high structural similarity between certain analytes.³⁰ Evidently, an assay specific for the molecule of interest (*pCA*) is necessary to filter out gene targets that passed the initial screening for phenotypic readout (betaxanthin)-related reasons and not due to the improved AAA precursor supply.

2.3. Six Targets Significantly Improve p-CA Production. The industrial relevance of *pCA* has sparked intensive metabolic engineering campaigns aiming to develop *S. cerevisiae* strains capable of producing this aromatic compound at high levels. To the best of our knowledge, the strain developed by Liu et al. reaching 12.5 g/L *pCA* in a controlled fed-batch fermentation is the highest reported production titer to date.¹⁴ As such, many rational genetic engineering targets

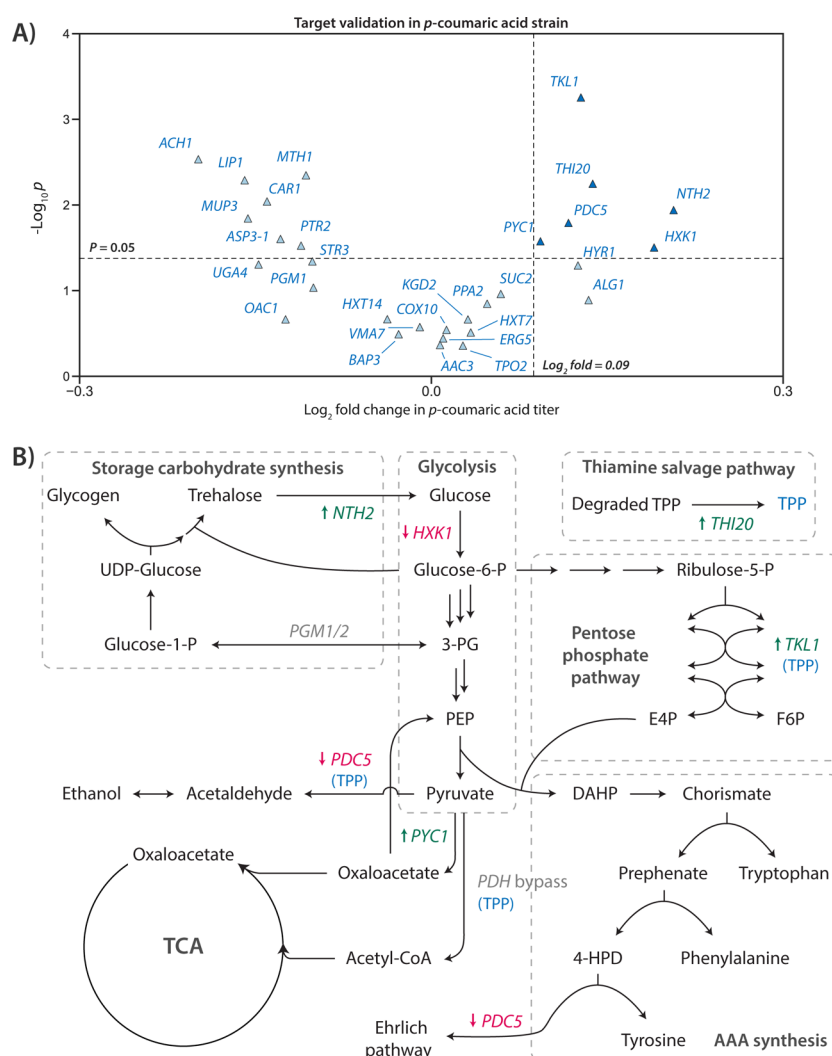


Figure 4. Target validation in a *p*-coumaric acid platform strain and the proposed metabolic involvement of the beneficial targets in *S. cerevisiae*. (A) Validation of the 30 unique genetic targets identified by screening of the dCas9-Mxi and dCas9-VPR betaxanthin yeast libraries for improving *p*CA production. The selection cutoff was Log_2 fold change >0.09 , and *p*-value <0.05 as represented by dark blue triangles, and statistical significance was measured using Student's *t* test (one-tailed; two-sample unequal variance). (B) Reactions for the six genetic targets within the arbitrary cutoff as defined in A in connection to the native *S. cerevisiae* metabolism. Abbreviations of the metabolites: TPP, thiamine pyrophosphate; PDH, pyruvate decarboxylase; glucose-1-P, glucose-1-phosphate; 3-PG, glyceraldehyde 3-phosphate; see Figure 1 legend for the abbreviations of other metabolites.

that improve AAA supply in *S. cerevisiae* have already been uncovered. However, as strains are continually engineered for improved production, the identification of additional beneficial targets further improving production becomes increasingly challenging due to negative epistasis.³¹ Accordingly, we decided to screen and validate our 30 genetic targets in a state-of-the-art *p*CA strain containing many, but not all, of the modifications in Liu et al., both to ensure their relevancy to current efforts in rewiring metabolism to AAA production, but also to ensure that production was sufficient to resolve marginal improvements in *p*CA titer. Specifically, compared to the strain by Liu et al., the *p*CA strain generated in this study lacks galactose inducible promoters driving heterologous gene expression, *GAL7/1/10* and *GAL80* disruption, and down-regulation of *PFK1/2* and *PYK1*, and is haploid. The genetic modifications required to establish the *p*CA validation strain for this study can be found in Figure 1B.

The 30 sgRNA plasmids extracted from the FACS-enriched isolates were transformed into the *p*CA strain, the resulting 30 strains were cultivated, and *p*CA production was quantified

(Figure 2B). As expected, both due to differences in the Btx and *p*CA genetic backgrounds and shortcomings related to using betaxanthin as a readout for AAA, only six of the targets improved *p*CA production with a cutoff of *p*CA titer fold improvement >1.06 , corresponding to a Log_2 fold improvement >0.09 , and *p*-value <0.05 . These final targets constitute the clones with perturbations in the expression level of the six genes: pyruvate carboxylase *PYC1*, pyruvate decarboxylase *PDC5*, transketolase *TKL1*, the trifunctional enzyme of thiamine biosynthesis, degradation, and salvage *THI20*, hexokinase *HXK1*, and trehalase *NTH2*. The improvement in *p*CA titer for these targets after 48 h cultivation in the batch mineral medium was: 6% for *PYC1*, 8% for *PDC5*, 9% for *TKL1*, 10% for *THI20*, 14% for *HXK1*, and 15% for *NTH2* (Figure 4A and Supplementary File 1, Figure S3). Although not statistically significant, we interestingly also saw that *ALG1* (highest occurrence in betaxanthin screening) on average also improved *p*CA production. Accordingly, we have demonstrated that less-specific HTP assays can provide a filtered list of genetic targets that subsequently can be validated in a

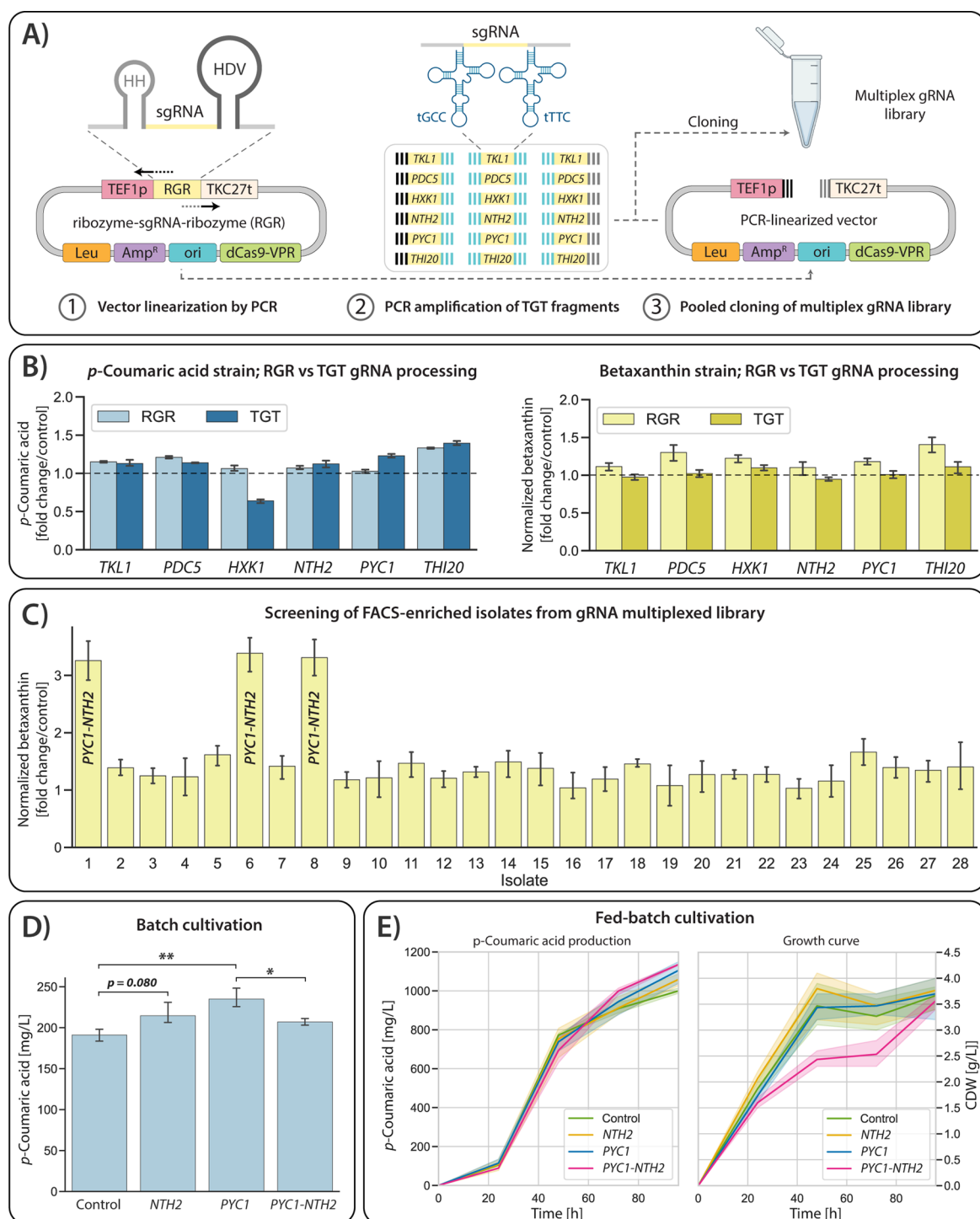


Figure 5. Multiplexed gRNA library construction and screening. (A) Schematic overview of the workflow for switching the gRNA processing method from ribozyme-sgRNA-ribozyme (RGR) to the tRNA-sgRNA-tRNA (TGT) system and constructing the multiplexed gRNA library. (B) Comparison of the performance for single-target perturbations with RGR and TGT processing methods in both *p*CA and Btx strains. (C) Fold change of normalized fluorescence over the betaxanthin screening strain without a gRNA for 28 single clones isolated from the sorted multiplexed-TGT-library in the Btx strain. The data were taken after 48 h of growth for $n = 4$ biologically independent samples. (D) Results of *p*CA titer after 48 h in strains with single and multiplexed TGTs targeting *PYC1* and *NTH2* in batch medium (shake flasks) supplemented with 20 g/L glucose. (E) *p*CA production titers for strain with multiplexed TGTs in fed-batch medium (shake flasks) with six tablets of FeedBeads in mineral medium after 96 h. All data represent mean values for $n = 3$ biologically independent samples. Statistical analysis in panel D was performed using one-way ANOVA and Tukey's HSD test ($*p < 0.05$, $**p < 0.01$).

specific LTP assay, here for identifying targets, improving AAA supply by proxy of *p*CA.

TKL1 and *PDC5* are well-established rational metabolic engineering targets for redirecting metabolic flux toward the

shikimate pathway. For instance, *TKL1* overexpression has been found to positively contribute to the production of aromatic compounds by improving E4P supply.³² While Liu et al. found that overexpression of *TKL1* decreased *p*CA

production, this could easily be due to differences in the genetic backgrounds of the *pCA*-producing strains.¹⁴ Similarly, blocking the degradation pathway (i.e., Ehrlich pathway) of AAAs and the cytosolic route to acetaldehyde by *PDC5* knockout has been shown to be an efficient method for rewiring the metabolic pathway toward AAA supply in yeast.^{33,34} However, in our *pCA* strain the *PDC5* gene had already been knocked out by complete ORF deletion (Figure 1C), so the enrichment of this target with the sgRNA loci at +80 bp of the start codon was initially perplexing. As gRNA targeting of the CRISPR/Cas9 system is known to have off-target cleavage activity on DNA with even 3–5 base pair mismatches in the PAM-distal part of the sgRNA sequence,³⁵ we looked into potential off-target sites for this particular gRNA target sequence. Here, we performed a BLASTn-short search of the sgRNA target sequence against the reference genome of CEN.PK113–7D (see File 1, Figure S4 and Table S7). The results showed 87.0% and 91.3% homology of the sgRNA target sequence to genes *PDC1* and *ARO10*, respectively. The binding sites were also around +80 and +140 bp downstream the start codon of the *PDC1* and *ARO10* genes, respectively, and importantly the Cas9 PAM site “NGG” was preserved in both off-target sites. As *ARO10* was likewise disrupted in the *pCA*-screening strain, it seems possible that through off-target activity of the +80 *PDC5* sgRNA, *PDC1* was indeed regulated instead—and the observed improvement in *pCA* production was caused by *PDC1* repression. *PDC5* and *PDC1* are key enzymes in the alcoholic fermentation of *S. cerevisiae*—first degrading pyruvate into acetaldehyde, which is then converted into ethanol. While *PDC5* and *PDC1* cannot be disrupted simultaneously without significantly impairing growth,^{36,37} our results indicate that *PDC1* knockdown paired with *PDC5* disruption may be an effective strategy for further improving AAA production without growth impairment. The off-target activity of the +80 *PDC5* sgRNA also makes it quite likely that all three genes, i.e., *PDC1*, *PDC5* and *ARO10* were simultaneously repressed through this mechanism in the betaxanthin strain (three occurrences), as in this strain the genes were present in the genome.

The enrichment of isolates with perturbed expression levels of *HXK1* and *PYC1* might be the most relevant from a literary perspective, as the flux balance between the glycolysis and the PPP has been described as a crucial branching point for directing flux into the shikimate pathway.^{14,38} The enrichment of *HXK1* repression in our screen is likely due to the resulting alleviation of *HXK2* repression, as these two hexokinase isoenzymes have been found to impose feedback inhibition on each other.^{39–41} *HXK2* is the predominant kinase in the glucose catabolism of *S. cerevisiae* and a global regulator of carbon metabolism essential in glucose repression signaling,⁴² and so alleviated repression of *HXK2* could lead to an increase in glucose phosphorylation and enhanced flux through glycolysis. The enrichment of *PYC1* activation in our screen is surprising, as Cai et al. reported a downregulation of *PYC1* in mutants with improved L-tyrosine production.²⁰ While *PYC1*'s involvement in the AAA metabolism is still largely speculative, it seems plausible that it improves AAA precursor supply by recovering pyruvate through gluconeogenesis, converting it into PEP that can subsequently enter the shikimate pathway (see Figure 4B). The synthesis of storage carbohydrates, i.e., glycogen and trehalose, is vital for cell survival and proliferation during nutritional and thermal stresses⁴³ but also drains the intracellular Glc-6-P, reducing the availability of

this compound for glycolysis and/or PPP routes. As such, an upregulated trehalase *NTH2* would increase the metabolite pool in the glycolysis pathway and as a result further improve AAA production. Thiamine and its phosphorylated biologically active forms are important cofactors in central metabolism, such as in glycolysis and the PPP.⁴⁴ Notably, transketolases (e.g., *TKL1*) and phosphoketolases (e.g., *Bbx1pk*) both employ thiamine pyrophosphate (TPP) as a cofactor. Accordingly, the activation of *THI20* likely improves AAA production by increasing the availability of TPP as a cofactor for the native and heterologous transketolases driving E4P production.

2.4. Additive Interaction of *PYC1* and *NTH2* Identified by a Multiplexed gRNA Library. The implementation of transcriptional regulatory gRNA libraries coupled to a Btx/*pCA* production-based screening enabled the identification of six distinct gene targets whose modulated expression resulted in improved *pCA* levels. Since cellular metabolism is highly regulated by complex regulatory networks, genetic targets often need to be perturbed in unison and to a specific degree to rewire metabolism to the desired phenotype. As such, while identifying single gene targets in heavily engineered strains is certainly challenging, it pales in comparison to the difficulty of finding compatible targets that additively improve production. It has been estimated that many genetic targets are subject to epistasis⁴⁵ and consequently single-target engineering efforts often lead to diminishing returns and saturation when targets are combined.^{46–48} We were therefore curious if any of the six targets identified to improve *pCA* production could be combined to additively improve AAA production further. To this end, we initially switched the current ribozyme-sgRNA-ribozyme (RGR) sgRNA processing system to the endogenous RNA processing tRNA-sgRNA-tRNA (TGT) system that has been shown to support simultaneous disruption of up to 8 genes with 87% efficiency (Figure 5A).^{49,50} In contrast, the limited cleavage capacity of the native *S. cerevisiae* ribozyme system (RGR) only supports the efficient processing of four tandem sgRNAs,⁴⁸ and we would like a system that at least in theory allows all six of our single-target gRNAs to be assembled and processed from a single transcript.

To assess the regulatory impact of switching to another gRNA processing system on our target genes, we comparatively cultivated Btx and *pCA* strains containing single gRNAs with either the ribozyme (RGR) or the tRNA (TGT)-based system (Figure 5B). Here, we interestingly observed that in the *pCA* strain, the TGT system was generally comparable to the RGR system across genetic targets, with the exception of *HXK1*, where the resulting *pCA* production was significantly lower. On the other hand, in the Btx strain mainly the gRNAs utilizing the RGR system were able to perturb the target genes to the desired phenotypic effect. To maximize our chances of finding synergistic interactions among the six *pCA* targets, we designed a multiplexed gRNA library to be fully combinatorial, in such a way that TGT units could assemble in any position relative to the *TEF 1p* promoter (Figure 5A). In this way, we would be able to rapidly test every combination of the six *pCA* targets without cloning the multiplexed gRNAs individually. Once cloned, we implemented the multiplexed TGT gRNA library in our betaxanthin screening strain and sorted for isolates with enhanced fluorescence compared to the betaxanthin screening strain. Here, we identified three isolates with more than a threefold improvement in betaxanthin production (Figure 5C), and sequencing revealed that they all contained sgRNAs targeting *PYC1-NTH2* (in that order). To

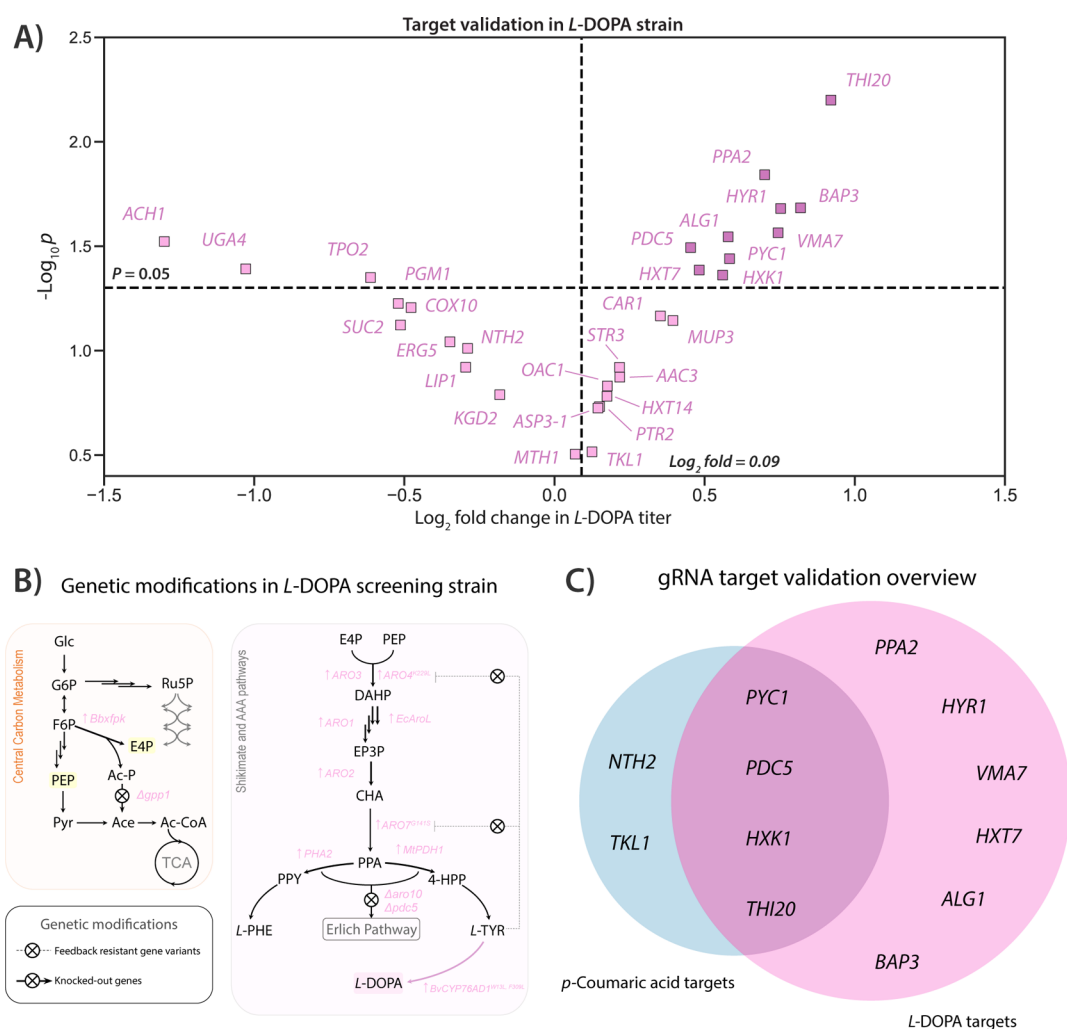


Figure 6. Further target validation in a L-DOPA platform strain and overview of genetic targets improving the production of L-DOPA and/or *p*-coumaric acid. (A) Validation of the 30 unique genetic targets identified by screening of the dCas9-Mxi and dCas9-VPR betaxanthin yeast libraries for improving L-DOPA production. The data were taken after 48 h of growth for $n = 2$ biologically independent samples, and statistical significance was measured using Student's *t* test (one-tailed; two-sample unequal variance). The selection cutoff was Log_2 fold change >0.09 and p -value <0.05 as represented by dark purple squares. (B) Genetic modifications implemented in *S. cerevisiae* metabolism for generating the L-DOPA screening strain. The L-DOPA screening strain contains the same genetic modifications to native metabolism as the *p*CA strain. (C) Venn diagram of the genetic targets that significantly improved the production of L-DOPA and/or *p*CA. See Figure 1 legend for the abbreviations of metabolites.

verify that *PYC1-NTH2* perturbed simultaneously would have a positive epistatic effect on AAA production, we introduced multiplexed gRNA in the *p*CA validation strain. Cultivated in batch conditions (shake flasks), the additive effect was not transferable to *p*CA production (Figure 5D). Additionally, we observed a discrepancy in *p*CA production in shake flasks compared to 24-deep-well plates (see Figure 4A and Supplementary File 1, Figure S3), with *PYC1* (23.0% improvement) here outperforming *NTH2* (12.4% improvement).

As *PYC1* and *NTH2* both participate in gluconeogenesis/famine, we speculated that cultivation conditions and carbon availability were perhaps important for manifestation of their positive epistatic interaction on *p*CA production. We therefore recultivated the strain in FeedBead medium mimicking fed-batch cultivation, which has been reported by Liu et al. to significantly improve AAA flux.¹⁴ Under these conditions (Figure 5E), we observed an additive trend when *PYC1* and *NTH2* were perturbed simultaneously, with 1135.2 ± 2.9 mg/L *p*CA produced in 96 h compared to 999.7 ± 11.1 mg/L in

the control strain (13.5% improvement, p -value = 0.001). While only statistically significant for *NTH2* (72 h, $NTH2 = 0.04$ & $PYC1 = 0.13$; 96 h, $NTH2 = 0.05$ & $PYC1 = 0.23$; one-tailed Student's *t* test with two-sample unequal variance), on average both at 72 and 96 h the multiplexed *PYC1-NTH2* gRNA outperformed the single-target gRNAs, suggesting a potential additive effect. Interestingly, we observed significantly slower growth (CDW) for the middle 48 h ($t = 24$ –72 h) of the cultivation for the strain containing the multiplexed gRNA, and since *p*CA production was largely unaffected (if not improved), the specific *p*CA titer for this strain is vastly superior for that duration of the cultivation (see Supplementary File 1, Figure S5).

2.5. Further Validation Reveals 10 Targets that Significantly Improve L-DOPA Production. Initial validation of the 30 genetic targets in a *p*CA-producing strain revealed six targets that significantly improved the level of *p*CA production. We chose *p*CA as our metabolite for LTP validation partly because it can be derived from both L-tyrosine and L-phenylalanine, thereby serving as a reliable

readout for the AAA supply. However, while our *pCA*-screening strain is able to convert both L-tyrosine and L-phenylalanine into *pCA*, Liu et al. reported that the production of *pCA* from L-phenylalanine is far more efficient (~26 fold) than from L-tyrosine.¹⁴ As betaxanthin is derived from L-tyrosine, we hypothesized that targets specifically improving L-tyrosine supply were being overlooked due to the inefficient conversion of L-tyrosine into *pCA*. To investigate this, we constructed a L-DOPA producing screening strain containing the same modifications to the native *S. cerevisiae* metabolism as our *pCA*-screening strain (Figure 6B). The 30 sgRNAs were then introduced in the L-DOPA strain, the resulting 30 strains cultivated in batch condition, and L-DOPA production quantified. Here, we found that 10 targets improved L-DOPA production with a cutoff L-DOPA titer fold improvement >1.06, corresponding to a Log₂ fold improvement >0.09, and *p*-value <0.05 (Figure 6A). Among these 10 targets, 4 (4/6) were also found to improve *pCA* production, namely, *PYC1*, *PDC5*, *HXK1*, and *THI20* (Figure 6C). *THI20* activation resulted in the largest improvement of L-DOPA production, increasing the secreted titer by ~89% (Log₂ fold change 0.92). We hypothesize that *THI20* activation improves AAA supply by increasing the availability of TPP as a cofactor for the native (*TKL1*) and heterologous (*Bbxfpk*) transketolases. Curiously, *NTH2* did not improve the production of L-DOPA, despite improving both the production of betaxanthin and *pCA* in previous cultivations. Our understanding of *NTH2*'s connection to AAA supply is limited, but it seems to be highly dependent on the target AAA-derived compound, the yeast genotype, and cultivation conditions. Six targets improved L-DOPA but not *pCA* production, namely, *PPA2*, *HYR1*, *VMA7*, *HXT7*, *ALG1*, and *BAP3*—and all by more than 36% (Log₂ fold change 0.45). While *HYR1* and *ALG1* on average also improved *pCA* production, this was not significant. The remaining four targets had little to no effect on *pCA* production. The six targets improving L-DOPA but not *pCA* production might have been excluded either due to the inefficient conversion of L-tyrosine to *pCA*, or because they specifically improve the L-DOPA biosynthesis pathway (*BvCYP76AD1*^{W13L,F309L}). This demonstrates that the list of targets acquired by our initial screening by proxy with betaxanthin can be used to improve the production of different metabolites from the same shared precursors.

3. DISCUSSION

The lack of HTP screening assays for the vast majority of interesting small molecules severely impedes metabolic engineering efforts. While artificial biosensors hold great promise for accelerating the “test” stage in the metabolic engineering cycle, the development of the biosensors themselves remains laborious. As a result, if a suitable biosensor does not exist, it is often more resource-efficient to pursue a metabolic engineering challenge rationally, rather than spending the resources on developing a specific biosensor and then pursuing the challenge with HTP engineering. In this study, we explored the promise of using betaxanthins, a widely used phenotypic readout for L-tyrosine, as an initial filter for genetic targets (summed library size: ~8000) that may improve AAA production in *S. cerevisiae*. We overcame the intrinsic issue of using betaxanthin directly as a readout by validating the targets in a LTP *pCA* assay, identifying six unique targets that significantly improved *pCA* production in an already heavily engineered strain. Hereafter, we generated a

multiplexed gRNA library of these six targets and identified an additive interaction between *PYC1* and *NTH2*. We further validated our “screening by proxy” workflow by testing the initial 30 targets in a L-DOPA platform strain, identifying 10 targets that significantly improved production. While the targets identified in this study are largely novel for improving AAA production in yeast, there are common themes in the metabolic nodes perturbed when compared to the literature. For instance, Liu et al. found that downregulating the pyruvate kinase *PYK1* improved *pCA* production, likely by reducing the conversion of PEP to pyruvate,¹⁴ and similarly we found that upregulating the pyruvate carboxylase *PYC1* improved *pCA* production, likely by increasing the conversion of pyruvate into oxaloacetate, which can be recovered into PEP under gluconeogenic conditions.

Regardless of biosensor specificity, the validation of the genetic targets in a strain producing the compound of interest is essential. That said, we imagine that the cutoff values for the initial filtered list of targets can be adjusted to be more or less selective depending on biosensor promiscuity—e.g., in our case, betaxanthin composition influenced fluorescence intensity and led to false positives. For instance, lowering the selection threshold from Log₂ fold change >1.8 to 1.5 might reduce the likelihood that true targets are excluded in favor of false ones. The trade-off of lowering the selection threshold is that it necessitates increased LTP target validation. Additionally, as our LTP screening evaluates only extracellular production, we imagine that fluorescence-assisted droplet sorting would provide better screening accuracy than FACS, although this requires microfluidic capabilities. AAA-specific yeast biosensors, e.g., Zhang et al. developed a L-tryptophan biosensor based on the *trpR* operon from *Escherichia coli* (*E. coli*), could be suitable alternatives to betaxanthin for screening AAA-enhancing targets by proxy, avoiding the false positives that often comes with betaxanthin-based screenings.⁵¹ To the best of our knowledge, a L-tyrosine-specific yeast biosensor has not yet been developed.

We propose that broad-range HTP assays sharing common precursors with the target compound can be useful as proxy for identifying nonintuitive beneficial modifications for compounds where HTP assays have not yet been developed. For instance, Zhang et al. recently developed yeast biosensors for the branch-chain amino acids (L-valine, L-leucine, and L-isoleucine), and we imagine a similar workflow as the one proposed here could be used to aid the production of the many valuable branch-chain amino acid-derived compounds.^{52,53}

The layered and intertwined regulatory networks governing amino acid biosynthesis make it difficult to identify and combine beneficial modifications in an additive manner in strains that have already been engineered. As we observed when switching the gRNA processing system prior to multiplexing (Figure 5B), presumably small changes in expression levels, e.g., for *THI20*, had a large impact on achieving the desired phenotype. Consequently, it is likely that the expression of many genes must be fine-tuned to a very specific level to get the desired effect, and this level is dependent on the state of the overall cellular metabolism and cultivation conditions. As the genetic context is rapidly changing in iterative metabolic engineering campaigns, it is likely that many targets remain overlooked due to our inability to fine-tune their expression appropriately. Similarly, as observed when cultivating the *PYC1* and *NTH2* multiplexed strain under batch and fed-batch conditions, it is crucial to

assess genetic modifications in different metabolic states—and ideally in conditions closely simulating the final application (if it is known, e.g., controlled fed-batch fermentations in bioreactors). However, fine-tuning expression levels at a genome-wide scale requires larger genetic libraries still—which ideally need to be screened in several conditions—and without efficient means to identify the desired phenotypes in HTP, such tools will be unviable. Biosensors for common precursors (e.g., individual amino acids) might be leveraged to initially filter genetic targets relevant for the biosynthetic production of a heterologous compound, without the need for a compound-specific biosensor. This filtered list of genetic targets can then be screened at varying expression levels, individually or in combination, and at different cultivation conditions to improve the probability of generating strains capable of performing well at the commercial manufacturing scale.

4. CONCLUSIONS

In this work, we demonstrated that less-specific HTP assays can be combined with specific LTP assays to identify nonintuitive genetic targets for molecules where artificial biosensors are not directly available. As a case study, we aimed at improving *p*-CA production in a *S. cerevisiae* strain by proxy of fluorescent L-tyrosine-derived betaxanthins, serving as a readout for the *p*-CA precursors (L-tyrosine and L-phenylalanine). Initial screening of transcriptional regulatory gRNA libraries revealed 30 genetic targets that significantly improved betaxanthin production. Subsequent validation in a *p*CA platform strain led to the identification of six targets that significantly improved *p*CA production. Additionally, we showed that this proxy workflow is useful for probing positive epistatic effects between genetic targets by generating a multiplexed gRNA library of the six targets, leading to the identification of an additive interaction between *PYCI* and *NTH2*. Finally, we further validated our “screening by proxy” workflow by testing the initial 30 targets in a L-DOPA platform strain, identifying 10 targets that significantly improved production. The development of compound-specific artificial biosensors is laborious, and this study demonstrates that screenable precursors to the compound of interest can be used as efficient proxies in HTP metabolic engineering campaigns to identify nonintuitive beneficial modifications.

5. MATERIALS AND METHODS

5.1. Strains and Media. *E. coli* strain DH5 α was used for cloning and plasmid propagation. The lysogeny broth (LB) liquid medium or LB solid medium supplemented with 20 g/L agar containing 100 mg/L ampicillin was used for *E. coli* cultivation at 37 °C. The strain CEN.PK 113-7D⁵⁴ was used as the yeast parent strain, and the subsequent strains listed in [Supplementary File 1, Table S1](#) were all derived from it.

The mineral medium used for cultivation of yeast strains was composed of 7.5 g/L (NH₄)₂SO₄, 14.4 g/L KH₂PO₄, 0.5 g/L MgSO₄·7H₂O, 2 mL/L trace metal (3.0 g/L FeSO₄·7H₂O, 4.5 g/L ZnSO₄·7H₂O, 4.5 g/L CaCl₂·2H₂O, 0.84 g/L MnCl₂·2H₂O, 0.3 g/L CoCl₂·6H₂O, 0.3 g/L CuSO₄·5H₂O, 0.4 g/L Na₂MoO₄·2H₂O, 1.0 g/L H₃BO₃, 0.1 g/L KI, and 19.0 g/L Na₂EDTA·2H₂O), and 1 mL/L vitamin solutions (0.05 g/L D-biotin, 1.0 g/L D-pantothenic acid hemicalcium salt, 1.0 g/L thiamin-HCl, 1.0 g/L pyridoxin-HCl, 1.0 g/L nicotinic acid, 0.2 g/L *p*-aminobenzoic acid, and 25.0 g/L *myo*-inositol). Due

to the interference of *p*-aminobenzoic acid in mineral media with quantification of betaxanthin fluorescence, we also prepared a modified mineral medium without *p*-aminobenzoic acid (*p*ABA[−]).

5.2. Plasmids, BioBricks, and Primers. All of the integration and gRNA vectors are listed in Supporting Information, [File 1, Table S2](#). The integration vectors were assembled by USER cloning according to the EasyClone MarkerFree method described by Jessop et al.⁵⁵ Correct assembly of the integration cassettes was verified by DNA sequencing (Eurofins Genomics, Germany). All BioBricks with templates and primers used for USER cloning are listed in [Supplementary File 1, Table S3](#), with primer sequences listed in [Supplementary File 1, Tables S4 and S5](#). For the amplification of BioBricks, Phusion U polymerase from ThermoFisher Scientific was used. The integration vectors were linearized via NotI digestion (New England Biolabs) according to the manufacturer's instructions.

For tracking sgRNAs, the vectors expressing dCas9-based enzyme perturbation were isolated from selected yeast strains using the NucleoSpin kit from Macherey-Nagel. For this, an overnight culture of yeast cells was grown in 5 mL of SC-leu media. Plasmid purification was performed according to the kit instruction, except that the cells were lysed by adding 0.5 mm acid-washed glass beads and shaking for 40 s at 6500 rpm in Precellys R 24 homogenizer (Bertin Corp., Montigny-le-Bretonneux, France). The purified plasmids were then transformed into *E. coli* DH5 α cells. The vectors were subsequently purified from *E. coli* cells using the same kit and Sanger-sequenced by PR-27020 (Eurofins Genomic, Germany).

5.3. Construction of Screening Strains. The screening strains, i.e., the Btx-, *p*CA, and L-DOPA strains, were constructed by Cas9-mediated marker-less genome editing, EasyClone MarkerFree toolkit.⁵⁵ To express the Cas9 protein, episomal vector pCfB2312 with a kanamycin resistance marker was transformed into CEN.PK113-7D, to obtain strain ST7574. The yeast transformations were performed using the standard lithium acetate method.⁵⁶ Yeast transformants for base strains were selected on yeast extract peptone dextrose medium (10 g/L yeast extract, 20 g/L peptone, 20 g/L glucose) supplemented with antibiotics nourseothricin (Jena Bioscience GmbH) at 100 mg/L, to select for strains harboring the gRNA vector, and G418 (Sigma-Aldrich) at 200 mg/L, to maintain selection for the Cas9 expression vector.

5.4. Construction of Yeast Libraries. To construct the yeast libraries from the dCas9-VPR or dCas9-Mxi1 plasmid libraries, the Btx screening strain (ST9633) was grown in 50 mL of YPD medium at 30 °C and 250 rpm for 5 h to get an optical density (OD) of 1.9–2.1. Each culture (25 mL) was used to transform the dCas9 vector libraries using the lithium acetate method.⁵⁵ After library transformation, the cells were grown overnight in 25 mL of synthetic complete media without leucine (SC-leu) to select cells successfully transformed with library vectors. The cultures were then diluted 1:10 to 5 mL of mineral medium. The rest of the cultures were mixed 1:1 with 50% glycerol and stored at −80 °C. The next day, the cultures were diluted 1:50 to 5 mL of mineral medium and grown overnight. This culture was used for library sorting.

5.5. Flow Cytometry and Library Sorting. To remove secreted betaxanthins, the yeast cells were washed twice with phosphate-buffered saline (PBS) buffer (pH 7.5) by centrifuging at 3000 × *g* for 5 min and finally resuspended in PBS

buffer. Library cells were then sorted by using the Sony SH800 Cell Sorter (Sony, Tokyo, Japan). The measurements were performed by using a 488 nm laser and a 525/50 band-pass filter. As cell doublets would significantly mislead the sorting experiments, events were first gated for singlets by discriminating single and double cells in SSC-width vs SSC-height. The gate size was set to capture approximately 50% of the population. Cells passing the singlet-selection gate were sorted for the top 1–3% of the fluorescence distribution. For each library, 10,000 events were sorted and collected in a culture tube containing 2 mL of mineral media and were grown overnight at 250 rpm and 30 °C. The sorting process was repeated once more for these cultures to ensure the enrichment of highly fluorescent single cells. The second-round sorted cells were plated on Nunc OmniTray™ single-well plates (Thermo Scientific) containing mineral medium agar, with a density of 3000–5000 events per plate. The plated cells were incubated at 30 °C for 4 days until single colonies were obtained (see Supplementary File 1, Figure S2).

5.6. Multiplexing sgRNAs. To generate a multiplexed sgRNA library from the single extracted sgRNAs, an empty dCas9-VPR destination vector (pCfB10875) was created by removing the sgRNA from any given single sgRNA via PCR and subsequent Gibson cloning. Here, the ribozyme-gRNA-ribozyme (RGR) unit was removed and replaced with a USER cloning site, and the library destination vector was verified by Sanger sequencing. The tRNA sequences (BB6131 and BB6132) were ordered as duplex oligomers from IDT, and the gRNA target sequences, including the gRNA scaffolds, were PCR amplified from the isolated RGR sgRNAs attaching Gibson overhangs compatible with the designed tRNA sequence. Hereafter, single tRNA-gRNA-tRNA (TGT) plasmids were generated by Gibson cloning and verified by Sanger sequencing. Using the single TGT plasmids as a template, each plasmid was amplified with primers generating USER-compatible overhangs with either the TEF 1p (unique), other TGT BioBricks (universal), or the TKC27t (unique)—e.g., for *TKL1* the following BioBricks were generated BB5526 (UniQ_TKL1_UniV), BB5527 (UniV_TKL1_UniV), and BB5528 (UniV_TKL1_UniQ). Hereafter, equal molar ratios of the TGT BioBricks were mixed, USER-digested, and subsequently ligated via T4 DNA ligase (30 min). The gRNA library destination vector was linearized with SfaAI and nicked with Nb.BsmI. The ligation mixture and linear destination vector were cloned into *E. coli* DH5 α . The TGT sgRNA library was incubated for 16 h in 4 mL of LB media supplemented with 100 mg/L ampicillin at 37 °C while being shaken (300 rpm), and then the cells were pelleted, and 25 mL of fresh LB media with 100 mg/L ampicillin was added. The library was incubated for another 16 h, pelleted, and resuspended in 1 mL of LB media with 100 mg/L ampicillin. Serial dilutions were made and plated to assess the library size, 150 μ L was inoculated into 4 mL of LB media with 100 mg/L ampicillin for purification of the library, and the remaining library was stocked at –80 °C.

5.7. Metabolite Production and Analytics. For fluorescence measurements, the cells were cultivated overnight in 96-deep-well plates containing 400 μ L of modified mineral medium (without *p*-aminobenzoic acid) with air-penetrable metal lids (EnzyScreen, The Netherlands) at 30 °C and 250 rpm. The next day, the cultures were diluted with fresh modified mineral media to get an OD of 0.1 and were incubated at 30 °C and 250 rpm for 48 h. The OD₆₀₀ and

fluorescence (485–515 nm) were measured in a plate reader (BioTek ELx 808) for $n = 6$ biological replicates, and data are reported as fluorescence/OD₆₀₀.

For *p*CA and L-DOPA production, the strains were cultivated overnight in 5 mL of mineral medium in 13 mL tubes at 30 °C and 250 rpm. For batch mode *p*CA production, an adequate volume of cells was inoculated the following day into 24-deep-well plates containing 2 mL of mineral media to get a starting OD₆₀₀ value of 0.1. The plates were cultivated at 30 °C and 250 rpm for 48 h, and the cultures were analyzed for dry cell weight (DCW) and *p*CA titer. For batch mode L-DOPA production, an adequate amount of overnight cultured cells was inoculated to 96-deep-well plates containing 400 μ L of mineral media supplemented with 10 mM ascorbic acid (to prevent L-DOPA oxidation). The starting OD₆₀₀ value of these cultures was 0.1, and the plates were cultivated at 30 °C and 250 rpm for 48 h. For the fed-batch mode of *p*CA synthesis, an adequate volume of overnight-grown cells was inoculated into 20 mL of mineral medium in 120 mL of un baffled shake flasks to get starting OD₆₀₀ of 0.1. To mimic fed-batch feeding, six tablets of FeedBeads (SMFB08001, Kuhner Shaker, Basel, Switzerland) were used in each culture. The flasks were then incubated at 30 °C with shaking at 200 rpm and samples were taken every 24 h. At the end of cultivation, samples were analyzed for DCW and *p*CA or L-DOPA titer.

The *p*CA and L-DOPA standards were purchased from Sigma-Aldrich with certified purity >96%. Quantification of *p*CA was performed with a Dionex Ultimate 3000 HPLC (ThermoFisher Scientific), equipped with a Zorbax column with particle size 5 μ m. The column oven temperature was set at 30 °C and the flow rate to 1 mL/min, with 10 μ L of sample injection. Solvent A was 0.1% formic acid, and solvent B was acetonitrile. Solvent composition was initially A = 80.0% and B = 20.0%, which was kept until 1 min. Then, the solvent composition was changed following a linear gradient until A = 60.0% and B = 40.0% at 2.0 min. These conditions were kept constant until 5.5 min. The retention time of *p*CA was 3.21 min, and the absorbance was measured at 310 nm.

The quantification of L-DOPA was done in a similar high-performance liquid chromatography (HPLC) system, using a sPPF column with the temperature maintained at 30 °C and the flow rate set to 0.3 mL/min, injecting 10 μ L of sample. Solvent A was 10 mM ammonia, and solvent B was acetonitrile. The solvent composition was initially 100.0% until 3.7 min. Then, the solvent composition was changed following a linear gradient until A = 30.0% and B = 70.0% at 4.0 min. These conditions were kept constant until 5.0 min, after which it was changed to A = 100.0% again at 5.2 min and kept constant until the end of the run at 13.0 min. The retention time of L-DOPA was 4.02 min, and the absorbance was measured at 280 nm. Analysis of HPLC results was performed using Chromeleon 7 software (ThermoFisher Scientific).

■ ASSOCIATED CONTENT

Supporting Information

The Supporting Information is available free of charge at <https://pubs.acs.org/doi/10.1021/acssynbio.3c00396>.

Overview of the chemical structural space of betaxanthins; sorted betaxanthin library on mineral medium agar plate; *p*-coumaric acid production for isolates containing the FACS-enriched sgRNAs; alignments of

the PDC5(+80) gRNA target sequence against the most significant hits (PDC1 and ARO10) from the BLASTn-short search; specific p-coumaric acid titer for the PYC1-NTH2 multiplexed gRNA in fed-batch conditions; all oligonucleotides, BioBricks, plasmids, and strains used and/or generated in this study; all codon-optimized nucleotide sequences and the corresponding amino acid sequences for the heterologous genes used in this study; and BLASTn-short search of the PDC5(+80) sgRNA target sequence against the reference genome of CEN.PK113-7D (PDF)

AUTHOR INFORMATION

Corresponding Author

Irina Borodina – Novo Nordisk Foundation Center for Biosustainability, Technical University of Denmark, 2800 Kgs. Lyngby, Denmark; Email: irbo@biosustain.dtu.dk

Authors

Mahsa Babaei – Novo Nordisk Foundation Center for Biosustainability, Technical University of Denmark, 2800 Kgs. Lyngby, Denmark; orcid.org/0000-0002-7862-0811

Philip Tinggaard Thomsen – Novo Nordisk Foundation Center for Biosustainability, Technical University of Denmark, 2800 Kgs. Lyngby, Denmark; orcid.org/0000-0003-4498-4550

Marc Cernuda Pastor – Novo Nordisk Foundation Center for Biosustainability, Technical University of Denmark, 2800 Kgs. Lyngby, Denmark

Michael Krogh Jensen – Novo Nordisk Foundation Center for Biosustainability, Technical University of Denmark, 2800 Kgs. Lyngby, Denmark; orcid.org/0000-0001-7574-4707

Complete contact information is available at: <https://pubs.acs.org/10.1021/acssynbio.3c00396>

Author Contributions

M.B.: conceptualization, methodology, investigation, formal analysis, supervision, writing—original draft, and writing—review and editing. P.T.T.: conceptualization, methodology, investigation, formal analysis, writing—original draft, and writing—review and editing. M.C.P.: investigation and formal analysis. M.K.J.: conceptualization, supervision, and writing—review and editing. I.B.: conceptualization, supervision, writing—review and editing, and funding acquisition. M.B. and P.T.T. contributed equally.

Notes

The authors declare the following competing financial interest(s): IB, MB, PTT, and MCP are co-inventors on a patent application related to this research. The remaining authors declare no competing interests.

ACKNOWLEDGMENTS

This project has received funding from the European Union's Horizon 2020 research and innovation programme under grant nos. 814408 (SHIKIFACTORY100) and 757384 (YEAST-TRANS), The Novo Nordisk Foundation (grant nos. NNF20OC0060809, NNF20CC0035580, and NNF21OC0072559), and the US Department of Energy JGI Synthesis Program under FP0005685. The authors wish to

thank Guokun Wang and Vasil D'Ambrosio for their valuable discussions throughout the study.

REFERENCES

- (1) Garst, A. D.; Bassalo, M. C.; Pines, G.; Lynch, S. A.; Halweg-Edwards, A. L.; Liu, R.; Liang, L.; Wang, Z.; Zeitoun, R.; Alexander, W. G.; Gill, R. T. Genome-Wide Mapping of Mutations at Single-Nucleotide Resolution for Protein, Metabolic and Genome Engineering. *Nat. Biotechnol.* **2017**, *35* (1), 48–55.
- (2) Wang, G.; Møller-Hansen, I.; Babaei, M.; D'Ambrosio, V.; Christensen, H. B.; Darbani, B.; Jensen, M. K.; Borodina, I. Transportome-Wide Engineering of *Saccharomyces Cerevisiae*. *Metab. Eng.* **2021**, *64*, 52–63.
- (3) Bowman, E. K.; Deaner, M.; Cheng, J.-F.; Evans, R.; Oberortner, E.; Yoshikuni, Y.; Alper, H. S. Bidirectional Titration of Yeast Gene Expression Using a Pooled CRISPR Guide RNA Approach. *Proc. Natl. Acad. Sci. U.S.A.* **2020**, *117* (31), 18424–18430.
- (4) Wang, G.; Björk, S. M.; Huang, M.; Liu, Q.; Campbell, K.; Nielsen, J.; Joansson, H. N.; Petranovic, D. RNAi Expression Tuning, Microfluidic Screening, and Genome Recombineering for Improved Protein Production in *Saccharomyces Cerevisiae*. *Proc. Natl. Acad. Sci. U. S. A.* **2019**, *116* (19), 9324–9332.
- (5) Roy, K. R.; Smith, J. D.; Vonesch, S. C.; Lin, G.; Tu, C. S.; Lederer, A. R.; Chu, A.; Suresh, S.; Nguyen, M.; Horecka, J.; Tripathi, A.; Burnett, W. T.; Morgan, M. A.; Schulz, J.; Orsley, K. M.; Wei, W.; Aiyar, R. S.; Davis, R. W.; Bankaitis, V. A.; Haber, J. E.; Salit, M. L.; St. Onge, R. P.; Steinmetz, L. M. Multiplexed Precision Genome Editing with Trackable Genomic Barcodes in Yeast. *Nat. Biotechnol.* **2018**, *36* (6), 512–520.
- (6) Li, Y.; Mensah, E. O.; Fordjour, E.; Bai, J.; Yang, Y.; Bai, Z. Recent Advances in High-Throughput Metabolic Engineering: Generation of Oligonucleotide-Mediated Genetic Libraries. *Biotechnology Advances* **2022**, *59*, No. 107970.
- (7) Yu, W.; Xu, X.; Jin, K.; Liu, Y.; Li, J.; Du, G.; Lv, X.; Liu, L. Genetically Encoded Biosensors for Microbial Synthetic Biology: From Conceptual Frameworks to Practical Applications. *Biotechnol. Adv.* **2023**, *62*, No. 108077.
- (8) Koch, M.; Pandi, A.; Borkowski, O.; Batista, A. C.; Faulon, J.-L. Custom-Made Transcriptional Biosensors for Metabolic Engineering. *Curr. Opin. Biotechnol.* **2019**, *59*, 78–84.
- (9) Qiu, C.; Zhai, H.; Hou, J. Biosensors Design in Yeast and Applications in Metabolic Engineering. *FEMS Yeast Research* **2019**, *19* (8), No. foz082.
- (10) Xu, J.-J.; Fang, X.; Li, C.-Y.; Yang, L.; Chen, X.-Y. General and Specialized Tyrosine Metabolism Pathways in Plants. *aBIOTECH* **2020**, *1* (2), 97–105.
- (11) Aversch, N. J. H.; Krömer, J. O. Metabolic Engineering of the Shikimate Pathway for Production of Aromatics and Derived Compounds—Present and Future Strain Construction Strategies. *Front. Bioeng. Biotechnol.* **2018**, *6*, 32 DOI: [10.3389/fbioe.2018.00032](https://doi.org/10.3389/fbioe.2018.00032).
- (12) Cao, M.; Gao, M.; Suástegui, M.; Mei, Y.; Shao, Z. Building Microbial Factories for the Production of Aromatic Amino Acid Pathway Derivatives: From Commodity Chemicals to Plant-Sourced Natural Products. *Metabolic Engineering* **2020**, *58*, 94–132.
- (13) Huccetogullari, D.; Luo, Z. W.; Lee, S. Y. Metabolic Engineering of Microorganisms for Production of Aromatic Compounds. *Microb. Cell Fact.* **2019**, *18*, 41 DOI: [10.1186/s12934-019-1090-4](https://doi.org/10.1186/s12934-019-1090-4).
- (14) Liu, Q.; Yu, T.; Li, X.; Chen, Y.; Campbell, K.; Nielsen, J.; Chen, Y. Rewiring Carbon Metabolism in Yeast for High Level Production of Aromatic Chemicals. *Nat. Commun.* **2019**, *10* (1), 4976.
- (15) Bowman, E. K.; Wagner, J. M.; Yuan, S.-F.; Deaner, M.; Palmer, C. M.; D'Oelsnitz, S.; Cordova, L.; Li, X.; Craig, F. F.; Alper, H. S. Sorting for Secreted Molecule Production Using a Biosensor-in-Microdroplet Approach. *Proc. Natl. Acad. Sci. U. S. A.* **2021**, *118* (36), No. e2106818118.

- (16) Jiang, T.; Li, C.; Yan, Y. Optimization of a P-Coumaric Acid Biosensor System for Versatile Dynamic Performance. *ACS Synth. Biol.* **2021**, *10* (1), 132–144.
- (17) Siedler, S.; Khatri, N. K.; Zsoshár, A.; Kjærboelling, I.; Vogt, M.; Hammar, P.; Nielsen, C. F.; Marienhagen, J.; Sommer, M. O. A.; Joensson, H. N. Development of a Bacterial Biosensor for Rapid Screening of Yeast P-Coumaric Acid Production. *ACS Synth. Biol.* **2017**, *6* (10), 1860–1869.
- (18) DeLoache, W. C.; Russ, Z. N.; Narcross, L.; Gonzales, A. M.; Martin, V. J. J.; Dueber, J. E. An Enzyme-Coupled Biosensor Enables (S)-Reticuline Production in Yeast from Glucose. *Nat. Chem. Biol.* **2015**, *11* (7), 465–471.
- (19) Savitskaya, J.; Protzko, R. J.; Li, F.-Z.; Arkin, A. P.; Dueber, J. E. Iterative Screening Methodology Enables Isolation of Strains with Improved Properties for a FACS-Based Screen and Increased L-DOPA Production. *Sci. Rep.* **2019**, *9* (1), 1–10.
- (20) Cai, M.; Wu, Y.; Qi, H.; He, J.; Wu, Z.; Xu, H.; Qiao, M. Improving the Level of the Tyrosine Biosynthesis Pathway in *Saccharomyces Cerevisiae* through HTZ1 Knockout and Atmospheric and Room Temperature Plasma (ARTP) Mutagenesis. *ACS Synth. Biol.* **2021**, *10* (1), 49–62.
- (21) Smith, J. D.; Suresh, S.; Schlecht, U.; Wu, M.; Wagih, O.; Peltz, G.; Davis, R. W.; Steinmetz, L. M.; Parts, L.; St. Onge, R. P. Quantitative CRISPR Interference Screens in Yeast Identify Chemical-Genetic Interactions and New Rules for Guide RNA Design. *Genome Biol.* **2016**, *17* (1), 45.
- (22) Luttik, M. A. H.; Vuralhan, Z.; Suij, E.; Braus, G. H.; Pronk, J. T.; Daran, J. M. Alleviation of Feedback Inhibition in *Saccharomyces Cerevisiae* Aromatic Amino Acid Biosynthesis: Quantification of Metabolic Impact. *Metab. Eng.* **2008**, *10* (3–4), 141–153.
- (23) Khan, M. I.; Giridhar, P. Plant Betalains: Chemistry and Biochemistry. *Phytochemistry* **2015**, *117*, 267–295.
- (24) Gandía-Herrero, F.; García-Carmona, F. Biosynthesis of Betalains: Yellow and Violet Plant Pigments. *Trends Plant Sci.* **2013**, *18* (6), 334–343.
- (25) Gandía-Herrero, F.; García-Carmona, F.; Escribano, J. Development of a Protocol for the Semi-Synthesis and Purification of Betaxanthins. *Phytochemical Analysis* **2006**, *17* (4), 262–269.
- (26) Gandía-Herrero, F.; Escribano, J.; García-Carmona, F. Structural Implications on Color, Fluorescence, and Antiradical Activity in Betalains. *Planta* **2010**, *232* (2), 449–460.
- (27) Niziński, S.; Wendel, M.; Rode, M. F.; Prukala, D.; Sikorski, M.; Wybraniec, S.; Burdziński, G. Photophysical Properties of Betaxanthins: Miraxanthin V – Insight into the Excited-State Deactivation Mechanism from Experiment and Computations. *RSC Adv.* **2017**, *7* (11), 6411–6421.
- (28) Wendel, M.; Szot, D.; Starzak, K.; Tuwalska, D.; Gapinski, J.; Naskrecki, R.; Prukala, D.; Sikorski, M.; Wybraniec, S.; Burdziński, G. Photophysical Properties of Betaxanthins: Vulgaxanthin I in Aqueous and Alcoholic Solutions. *J. Lumin.* **2015**, *167*, 289–295.
- (29) Guerrero-Rubio, M. A.; Escribano, J.; García-Carmona, F.; Gandía-Herrero, F. Light Emission in Betalains: From Fluorescent Flowers to Biotechnological Applications. *Trends in Plant Science* **2020**, *25* (2), 159–175.
- (30) D'Ambrosio, V.; Pramanik, S.; Goroncy, K.; Jakočiūnas, T.; Schönauer, D.; Davari, M. D.; Schwaneberg, U.; Keasling, J. D.; Jensen, M. K. Directed Evolution of VanR Biosensor Specificity in Yeast. *Biotechnol. Notes* **2020**, *1*, 9–15.
- (31) Hong, K.-K.; Nielsen, J. Recovery of Phenotypes Obtained by Adaptive Evolution through Inverse Metabolic Engineering. *Appl. Environ. Microbiol.* **2012**, *78* (21), 7579–7586.
- (32) Curran, K. A.; Leavitt, J. M.; Karim, A. S.; Alper, H. S. Metabolic Engineering of Muconic Acid Production in *Saccharomyces Cerevisiae*. *Metabolic Engineering* **2013**, *15*, 55–66.
- (33) Rodríguez, A.; Kildegaard, K. R.; Li, M.; Borodina, I.; Nielsen, J. Establishment of a Yeast Platform Strain for Production of P-Coumaric Acid through Metabolic Engineering of Aromatic Amino Acid Biosynthesis. *Metab. Eng.* **2015**, *31*, 181–188.
- (34) Koopman, F.; Beekwilder, J.; Crimi, B.; van Houwelingen, A.; Hall, R. D.; Bosch, D.; van Maris, A. J. A.; Pronk, J. T.; Daran, J.-M. De Novo Production of the Flavonoid Naringenin in Engineered *Saccharomyces Cerevisiae*. *Microb. Cell Fact.* **2012**, *11*, 155.
- (35) Zhang, X.-H.; Tee, L. Y.; Wang, X.-G.; Huang, Q.-S.; Yang, S.-H. Off-Target Effects in CRISPR/Cas9-Mediated Genome Engineering. *Molecular Therapy - Nucleic Acids* **2015**, *4*, No. e264.
- (36) Ishida, N.; Saitoh, S.; Onishi, T.; Tokuhiko, K.; Nagamori, E.; Kitamoto, K.; Takahashi, H. The Effect of Pyruvate Decarboxylase Gene Knockout in *Saccharomyces Cerevisiae* on L-Lactic Acid Production. *Biosci. Biotechnol. Biochem.* **2006**, *70* (5), 1148–1153.
- (37) Wang, D.; Wang, L.; Hou, L.; Deng, X.; Gao, Q.; Gao, N. Metabolic Engineering of *Saccharomyces Cerevisiae* for Accumulating Pyruvic Acid. *Ann. Microbiol.* **2015**, *65* (4), 2323–2331.
- (38) Suástegui, M.; Guo, W.; Feng, X.; Shao, Z. Investigating Strain Dependency in the Production of Aromatic Compounds in *Saccharomyces Cerevisiae*. *Biotechnol. Bioeng.* **2016**, *113* (12), 2676–2685.
- (39) Palomino, A.; Herrero, P.; Moreno, F. Tpk3 and Snf1 Protein Kinases Regulate Rgt1 Association with *Saccharomyces Cerevisiae* HXK2 Promoter. *Nucleic Acids Res.* **2006**, *34* (5), 1427–1438.
- (40) Palomino, A.; Herrero, P.; Moreno, F. Rgt1, a Glucose Sensing Transcription Factor, Is Required for Transcriptional Repression of the HXK2 Gene in *Saccharomyces Cerevisiae*. *Biochem. J.* **2005**, *388*, 697–703.
- (41) Rodríguez, A.; De La Cera, T.; Herrero, P.; Moreno, F. The Hexokinase 2 Protein Regulates the Expression of the GLK1, HXK1 and HXK2 Genes of *Saccharomyces Cerevisiae*. *Biochem. J.* **2001**, *355* (Pt 3), 625–631.
- (42) Vega, M.; Riera, A.; Fernández-Cid, A.; Herrero, P.; Moreno, F. Hexokinase 2 Is an Intracellular Glucose Sensor of Yeast Cells That Maintains the Structure and Activity of Mig1 Protein Repressor Complex. *J. Biol. Chem.* **2016**, *291* (14), 7267–7285.
- (43) François, J. M.; Walther, T.; Parrou, J. L. Genetics and Regulation of Glycogen and Trehalose Metabolism in *Saccharomyces Cerevisiae*. In *Microbial Stress Tolerance for Biofuels: Systems Biology*; Liu, Z. L., Ed.; Springer Berlin Heidelberg: Berlin, Heidelberg, 2012; pp 29–55.
- (44) Bertels, L.-K.; Fernández Murillo, L.; Heinisch, J. J. The Pentose Phosphate Pathway in Yeasts—More Than a Poor Cousin of Glycolysis. *Biomolecules* **2021**, *11* (5), 725.
- (45) Kryazhinskiy, S. Emergence and Propagation of Epistasis in Metabolic Networks. *Elife* **2021**, *10*, No. e60200.
- (46) Deaner, M.; Alper, H. S. Systematic Testing of Enzyme Perturbation Sensitivities via Graded DCas9 Modulation in *Saccharomyces Cerevisiae*. *Metabolic Engineering* **2017**, *40*, 14–22.
- (47) Snitkin, E. S.; Segrè, D. Epistatic Interaction Maps Relative to Multiple Metabolic Phenotypes. *PLoS Genet* **2011**, *7* (2), No. e1001294.
- (48) Deaner, M.; Mejia, J.; Alper, H. S. Enabling Graded and Large-Scale Multiplex of Desired Genes Using a Dual-Mode DCas9 Activator in *Saccharomyces Cerevisiae*. *ACS Synth. Biol.* **2017**, *6* (10), 1931–1943.
- (49) Zhang, Y.; Wang, J.; Wang, Z.; Zhang, Y.; Shi, S.; Nielsen, J.; Liu, Z. A GRNA-TRNA Array for CRISPR-Cas9 Based Rapid Multiplexed Genome Editing in *Saccharomyces Cerevisiae*. *Nat. Commun.* **2019**, *10* (1), 1053.
- (50) McCarty, N. S.; Graham, A. E.; Studená, L.; Ledesma-Amaro, R. Multiplexed CRISPR Technologies for Gene Editing and Transcriptional Regulation. *Nat. Commun.* **2020**, *11* (1), 1281.
- (51) Zhang, J.; Petersen, S. D.; Radivojevic, T.; Ramirez, A.; Pérez-Manríquez, A.; Abeliuk, E.; Sánchez, B. J.; Costello, Z.; Chen, Y.; Fero, M. J.; Martin, H. G.; Nielsen, J.; Keasling, J. D.; Jensen, M. K. Combining Mechanistic and Machine Learning Models for Predictive Engineering and Optimization of Tryptophan Metabolism. *Nat. Commun.* **2020**, *11* (1), 4880.
- (52) Yu, A.-Q.; Pratomo Juwono, N. K.; Foo, J. L.; Leong, S. S. J.; Chang, M. W. Metabolic Engineering of *Saccharomyces Cerevisiae* for

the Overproduction of Short Branched-Chain Fatty Acids. *Metabolic Engineering* **2016**, *34*, 36–43.

(53) Zhang, Y.; Cortez, J. D.; Hammer, S. K.; Carrasco-López, C.; García Echaurren, S. A.; Wiggins, J. B.; Wang, W.; Avalos, J. L. Biosensor for Branched-Chain Amino Acid Metabolism in Yeast and Applications in Isobutanol and Isopentanol Production. *Nat. Commun.* **2022**, *13* (1), 270.

(54) Entian, K.-D.; Kötter, P. 25 Yeast Genetic Strain and Plasmid Collections. In *Methods in Microbiology*; Stansfield, I.; Stark, M. J., Eds.; Yeast Gene Analysis; Academic Press, 2007; Vol. 36, pp 629–666.

(55) Jessop-Fabre, M. M.; Jakočiūnas, T.; Stovicek, V.; Dai, Z.; Jensen, M. K.; Keasling, J. D.; Borodina, I. EasyClone-MarkerFree: A Vector Toolkit for Marker-Less Integration of Genes into *Saccharomyces Cerevisiae* via CRISPR-Cas9. *Biotechnol. J.* **2016**, *11* (8), 1110–1117.

(56) Gietz, R. D.; Schiestl, R. H. High-Efficiency Yeast Transformation Using the LiAc/SS Carrier DNA/PEG Method. *Nat. Protoc.* **2007**, *2* (1), 31–34.